

Title:

Magneto-Optical Imaging and Current Distributions in High-Tc Superconductors

Author(s):

A. Polyanskii, ASC, University of Wisconsin, Madison  
A. Pashitski, Inst. of Elec. Eng., Bratislava, Slovakia  
A. Gurevich, Inst. of Elec. Eng., Bratislava, Slovakia  
J.A. Parrell, Inst. of Elec. Eng., Bratislava, Slovakia  
M. Polak, Inst. of Elec. Eng., Bratislava, Slovakia  
D.C. Larbalestier, ASC, University of Wisconsin, Madison  
S.R. Foltyn, STC  
P.N. Arendt, MST-7

**MASTER**

Submitted to:

Advances in Superconductivity IX, Springer-Verlay, Tokyo  
Proceedings of the 9th International Symposium on Superconductivity (ISS 96')

10/21-24/96

HH

DISTRIBUTION OF THIS DOCUMENT IS UNLIMITED



**Los Alamos**  
NATIONAL LABORATORY

Los Alamos National Laboratory, an affirmative action/equal opportunity employer, is operated by the University of California for the U.S. Department of Energy under contract W-7405-ENG-36. By acceptance of this article, the publisher recognizes that the U.S. Government retains a nonexclusive, royalty-free license to publish or reproduce the published form of this contribution, or to allow others to do so, for U.S. Government purposes. The Los Alamos National Laboratory requests that the publisher identify this article as work performed under the auspices of the U.S. Department of Energy.

## DISCLAIMER

This report was prepared as an account of work sponsored by an agency of the United States Government. Neither the United States Government nor any agency thereof, nor any of their employees, make any warranty, express or implied, or assumes any legal liability or responsibility for the accuracy, completeness, or usefulness of any information, apparatus, product, or process disclosed, or represents that its use would not infringe privately owned rights. Reference herein to any specific commercial product, process, or service by trade name, trademark, manufacturer, or otherwise does not necessarily constitute or imply its endorsement, recommendation, or favoring by the United States Government or any agency thereof. The views and opinions of authors expressed herein do not necessarily state or reflect those of the United States Government or any agency thereof.

**DISCLAIMER**

**Portions of this document may be illegible in electronic image products. Images are produced from the best available original document.**

# MAGNETO-OPTICAL IMAGING AND CURRENT DISTRIBUTIONS IN HIGH- $T_c$ SUPERCONDUCTORS.

A. POLYANSKII<sup>1</sup>, A. PASHITSKI, A. GUREVICH, J.A. PARRELL, M. POLAK<sup>2</sup>,  
D.C. LARBALESTIER, S.R.FOLTYN<sup>3</sup>, AND P.N. ARENDT<sup>3</sup>.

Applied Superconductivity Center, University of Wisconsin, Madison, WI 53706, USA.

<sup>1</sup>Also at the Institute of Solid State Physics, Chernogolovka 142432, Russia.

<sup>2</sup>Also at the Institute of Electrical Engineering, Bratislava, Slovakia.

<sup>3</sup>Los Alamos National Laboratory, Los Alamos, NM 87545, USA.

## ABSTRACT

Recent studies on the magneto-optical (MO) imaging of the magnetic flux and current distributions in polycrystalline high- $T_c$  superconductors are summarized. We studied a wide spectrum of high- $T_c$  materials, from single grain boundaries in YBCO bicrystals, to polycrystalline YBCO thick films deposited on an IBAD-buffer layer grown on a polycrystalline Hastelloy substrate, to Bi-2223 tapes. In all cases we found that structural defects (e.g. high-angle grain boundaries, second phase precipitates, microcrack networks, etc.) significantly limit the current-carrying capability. These defects make the magnetic flux distribution highly inhomogeneous, in turn producing granular and percolative current flow. By inverting the Biot-Savart law for thin film and slab geometries, we were able to reconstruct the local current flow patterns around defects and thus identify the current-carrying percolative paths and map the distribution of local critical currents  $J_c(\mathbf{r})$ . Such studies show that, even in high- $J_c$  materials, the local  $J_c(\mathbf{r})$  can vary by a factor 2-10 due to defects. Since the maximum local  $J_c(\mathbf{r})$  values can significantly exceed the numbers obtained by transport measurements, it is clear that there are still significant opportunities for raising the  $J_c$  of polycrystalline HTS conductors.

KEY WORDS: Magneto-optical imaging, current distributions, percolation, structural defects, HTS.

## INTRODUCTION

Long length conductors for large scale applications of HTS require polycrystalline material forms, thus introducing the problem of poor grain-to-grain connectivity and the necessity of aligning the grains as well as possible in order to obtain high critical current density  $J_c$  [1]. It is well known that high-angle grain boundaries are practically opaque to supercurrent, as are other common current-limiting defects, such as microcracks and non-superconducting, second phase precipitates. As a result, the effective current-carrying cross-section in practical HTS materials can be very much less than the geometrical cross-section of the sample, since the current has to percolate through the defect network. In this case the current-carrying capability of HTS is determined by the distribution of current-limiting defects, rather than by intragrain flux pinning.

Recently, the current distributions  $\mathbf{J}(\mathbf{r})$  in polycrystalline HTS forms have been extensively studied by the magneto-optical (MO) imaging technique. When the images are quantified, the method enables one to extract  $\mathbf{J}(\mathbf{r})$  and  $H_z(\mathbf{r})$  maps in the vicinity of single grain boundaries in YBCO bicrystals [2] and to obtain the percolative distribution of magnetization and transport currents in Bi-tapes [3] and multifilament HTS conductors [4]. Used in qualitative mode, MO imaging enables the effect of unhealed deformation cracks to be directly proved. MO imaging proves to be a very valuable tool for quantifying the inhomogeneity of practical HTS materials and thus for revealing their significant potential for further improvement. In the following, we give characteristic examples taken from our recent work, which demonstrate the capabilities of MO imaging.

## RESULTS

### a. Current flow near a low angle grain boundary

Fig. 1 shows the MO image and the calculated current and field distributions around a low-angle, thin film  $5^\circ$  [001] tilt YBCO grain boundary grown on  $\text{SrTiO}_3$  by pulsed laser ablation. A nonzero critical current through the boundary ( $J_b$ ) results in a characteristic dark region in the center of the MO image which is clearly seen as a cusp in the pillow-like contours of the normal field  $H_z(\mathbf{r})$  observed above the surface. Fig. 1c shows the fields  $H_z(\mathbf{r})$  at a height of  $5 \mu\text{m}$  above the film calculated for the Bean-model current distribution of Fig. 1a. Excellent agreement between experiment and model was obtained [2]. The increase of the misorientation angle  $\theta$  above  $7^\circ$  results in a strong decrease of  $J_b(\theta)$ , so that no cusp in the MO image is then visible for  $\theta \geq 10^\circ$ . This is then the misorientation which effectively decouples the two grains of the bicrystal.

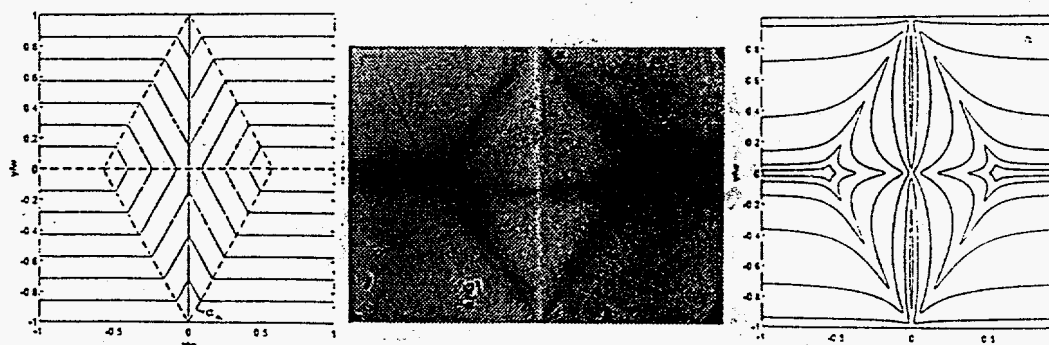


Fig. 1: a) Bean model current pattern for which half the intragrain current crosses the grain boundary. b) MO image of a  $5^\circ$  [001] tilt thin film YBCO bicrystal at 7 K and 72 mT. Darker regions correspond to lower local  $H_z(\mathbf{r})$  c) Computed contours of  $H_z(x,y)$  for the case shown in a) at a height  $\approx 5 \mu\text{m}$  above the surface (see Ref. [2] for details).

### b. Current flow in biaxially aligned YBCO tape

There has recently been great interest in methods of biaxially aligning YBCO on polycrystalline metallic substrates, using either the production of a quasi-single-crystal buffer layer of, for example, Yttrium-stabilized  $\text{ZrO}_2$  using Ion Beam Assisted Deposition (IBAD) [5,6] on a polycrystalline Hastelloy substrate or using a textured Ni substrate made by a rolling and subsequent heat treatment process [7]. The result is an overlayer YBCO film that has almost perfect c-axis texture with a very strong, but not perfect in-plane texture. The  $J_c(0 \text{ T}, 77 \text{ K})$  values can attain more than  $10^6 \text{ A/cm}^2$ , the exact value being strongly correlated to the distribution of the in-plane misorientation [6]. Fig. 2 shows the MO image of such a  $5 \times 0.3 \text{ mm} \times \approx 1 \mu\text{m}$  thick YBCO film made with an IBAD buffer layer on a polycrystalline Hastelloy substrate. The transport  $J_c(0 \text{ T}, 77 \text{ K})$  of this film was  $5 \times 10^5 \text{ A/cm}^2$ , consistent with a non optimum in-plane alignment. In such a case, the flux penetration and current distribution are inhomogeneous. We have recently developed methods to quantify the inhomogeneities of  $J_c(\mathbf{r})$ , using the scheme proposed in [8] for inverting the Biot-Savart law for thin film samples. A raw MO image, together with the derived current stream lines, are shown in Figs. 2a and 2b. The stream lines clearly show how the magnetization currents bypass low- $J_c$  regions, while the  $J_c$  map indicates significant variation of the local  $J_c(\mathbf{r})$  values. The spatial resolution of the technique in quantitative mode is of order  $5 \mu\text{m}$ , several times larger than the YBCO grain size. The fact therefore that  $J_c$  is varying by as much as by a factor of 10 in different parts of the sample seems to implicate the local grain-to-grain misorientation as being important for determining  $J_c$ . The best local  $J_c$  values (up to  $2 \text{ MA/cm}^2$ ) were about 4 times higher than the transport measurements.

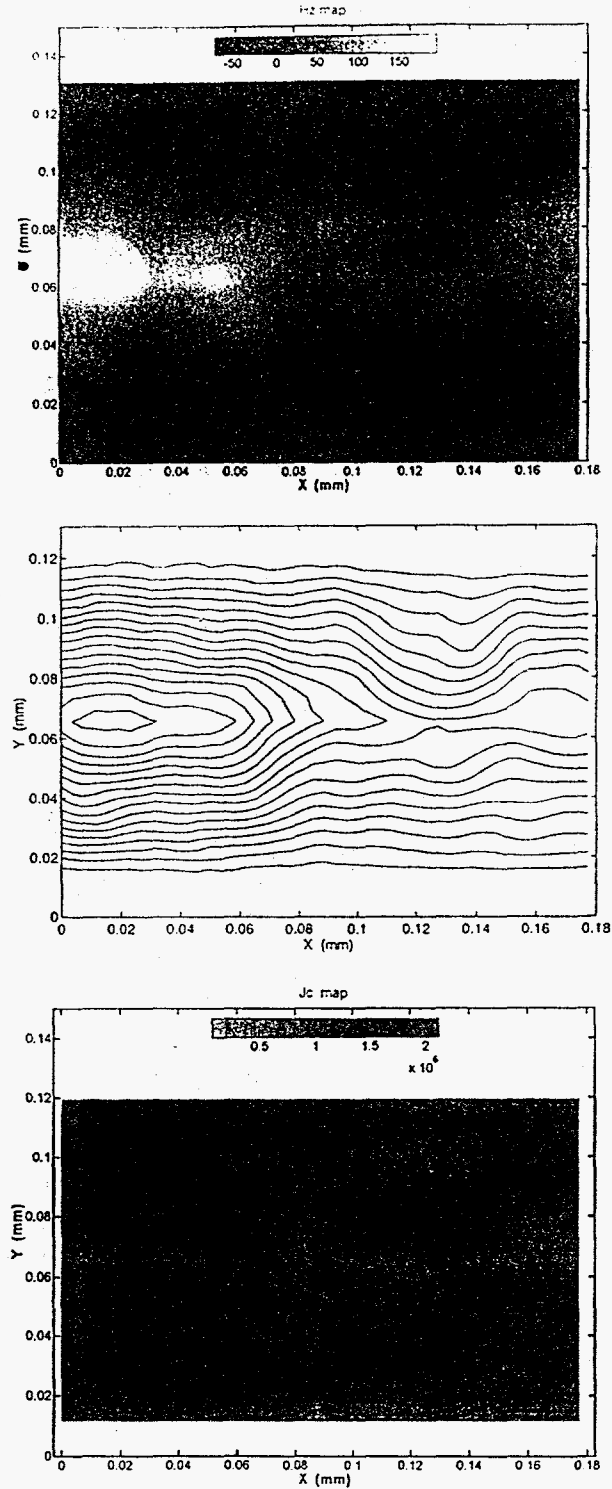


Fig. 2: a) MO image of trapped magnetic flux in a 1  $\mu\text{m}$  thick YBCO film made on an IBAD substrate. Darker regions correspond to higher local  $H_z(r)$  values. The image was obtained at 77 K after field cooling at  $H = 400$  Oe and then reducing  $H$  to zero; b) Reconstructed current stream lines for the image shown in a). The higher density of the stream lines corresponds to higher local  $J(r)$  values; c) Reconstructed  $J_c$ -map for the image shown in a). Darker colors correspond to higher local  $J(r)$  values according to the scale shown in the inset.

### c. Current limiting defects in BSCCO-2223 composites

It is abundantly clear from many experiments, particularly MOI experiments [3,4,9], that current flow in BSCCO composites is percolative. Although weak linked grain boundaries are clearly one cause for this, as exemplified by studies such as that shown for YBCO in Figs. 1 and 2, it is also clear that other types of barriers also exist. Polycrystalline BSCCO tapes differ strongly from YBCO in that they do not exhibit perfect c-axis texture (their in-plane texture is even worse), nor are they of full density. Thus thermal contraction mismatch, voids, large second phase particles and the deformation processes used to form a rolled tape all lead to crack networks that interrupt current flow. Recent experiments in our group have been very helpful in showing that these crack networks play a very important role in controlling the current flow in BSCCO tapes.

In a recent paper by Parrell et al. [10], the progressive changes that occur in the flux penetration as a tape is reacted through 3 heat treatments with intermediate pressing or rolling deformation steps were described. MOI images showed that there are distinct patterns to the flux penetration that depend on the number of heat treatments (HT) and on the type of deformation. The network of penetrating flux corresponds to all the weak links existing within the sample, whatever the source. Two networks appeared, one being approximately equiaxed and having a length scale of about 100  $\mu\text{m}$ , some 10 times the grain size, while the second was more linear and had an orientation that depended on whether the intermediate deformation step was by rolling or by pressing. In a development of this work by Polak et al. [11], the influence of bending strain on these networks was studied.

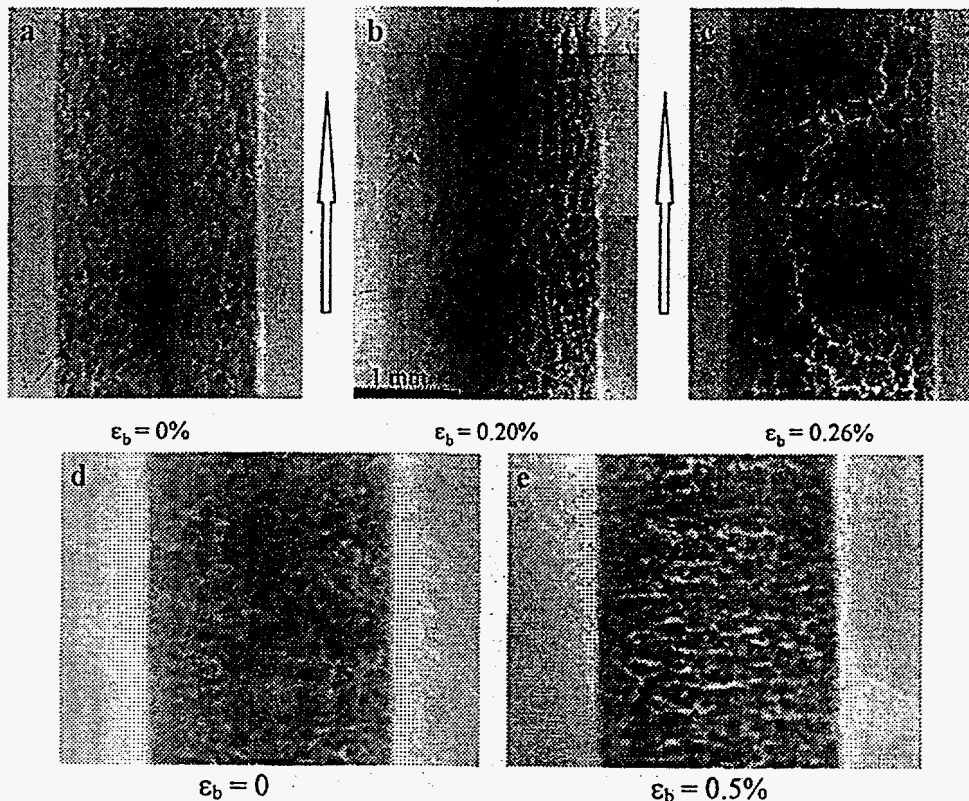


Fig. 3. MO images of pressed tapes (a) before bending and (b) after bending to  $\epsilon_b = 0.2\%$  and (c) after bending to  $\epsilon_b = 0.26\%$ ; MO images of rolled samples before (d) and after bending to  $\epsilon_b = 0.5\%$  (e).

The principal aspects of this work are visible in the data shown in Fig. 3. The linear networks of cracks are seen to be parallel to the tape axis in the case of pressed samples (see Fig. 3a, 3b, and 3c), while they appear to be normal to the tape axis for rolled samples (see Fig. 3d and 3e). These two flux penetration orientations correspond exactly to those predicted from analysis of the principal cracking directions during deformation [12]. We thus conclude that it is quite possible for cracks to be left unhealed by heat treatment, even when as many as three HT are given. These cracks not only interrupt current flow in the final heat treated state but they also act as the nucleation sites for cracking under subsequent bend deformation, as is shown by the bend strain pictures in Fig. 3: The principal cracks are seen to first propagate longitudinally for the pressed samples (compare Fig. 3a and 3b), but when the strain becomes large enough then cracks propagate out in a transverse direction, as expected from the state of stress (see Fig. 3c). In the case of reverse-bent rolled samples, both the initial and the bend-induced stresses cracks are transverse to the tape axis (see upper pair of MO images).

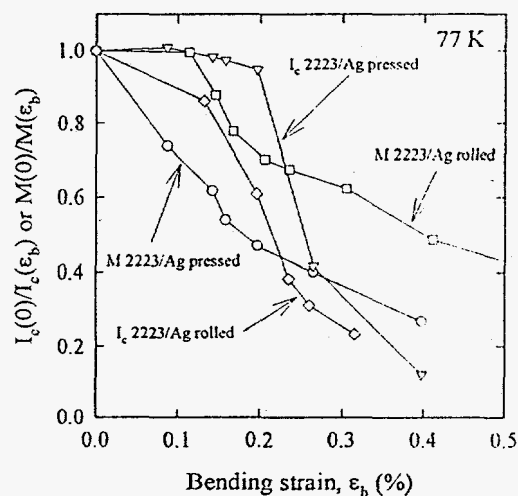


Fig. 4. Normalized magnetization and critical current as a function of bending strain for both pressed and rolled 2223 tapes.

samples, and while just a small number of transverse cracks can cause a great reduction of  $I_c$  measured along the longitudinal direction, they have a lesser effect on the magnetization currents. Straining pressed samples causes cracks to propagate in the longitudinal direction, which strongly effects the magnetization but does not greatly influence  $I_c$  measured along the same direction. Experiments like these illustrate the important role connectivity can play in determining  $J_c$  in polycrystalline Bi-2223 tapes.

## CONCLUSION

Our results indicate that various structural defects play a key role in determining the current-carrying capability of HTS conductors. The defects qualitatively change the character of current distribution, giving rise to a percolative, granular current flow. The very wide distribution of local  $J_c$  values reconstructed from MO images suggests that current carrying capability of polycrystalline HTS conductor forms can be significantly improved by eliminating particular structural defects.

The work at the University of Wisconsin was supported by EPRI, ARPA and by NSF. The work at LANL was supported by DOE.

The magnetization and transport data shown in the graph of Fig. 4 are consistent with the MO images, bearing in mind that transport current flows only axially along the tape while magnetization currents must flow both along and across the tape. The sample set exhibiting the least fall off in  $I_c$  with increasing strain is the pressed, transport current set. There is a distinct threshold for damage for this set, which is qualitatively consistent with the data of Fig. 3a and 3b. The rolled sample set exhibits no threshold and  $I_c$  declines distinctly more rapidly than it does for the pressed set. The magnetization data falls off more rapidly at low strains than does the transport data for pressed samples, but for the rolled samples the opposite occurs. This is due to the effect of the orientation of the residual microcrack network in pressed and rolled tapes, and how the cracks propagate when the tapes are strained. Small strains cause the propagation of transverse cracks in rolled



## REFERENCES

- <sup>1</sup> D.C. Larbalestier. To appear in *Proc. of 10th Anniversary HTS Workshop on Physics, Materials and Applications*, Houston, TX, March 11-14, 1996 (World Scientific 1996).
- <sup>2</sup> A. Polyanskii, A. Gurevich, A.E. Pashitski, N.F. Heimig, R.D. Redwing, J.E. Nordman, and D.C. Larbalestier, *Phys. Rev. B* **53**, 8687 (1996).
- <sup>3</sup> A.E. Pashitski, A. Polyanskii, A. Gurevich, J.A. Parrell, and D.C. Larbalestier, *Physica C* **246**, 133 (1995); *Appl. Phys. Lett.* **67**, 2720 (1995).
- <sup>4</sup> U. Welp, D.O. Gunter, G.W. Crabtree, J.S. Luo, V.A. Maroni, W.L. Carter, V.K. Vlasko-Vlasov, and V.I. Nikitenko, *Appl. Phys. Lett.* **66**, 1271 (1995); U. Welp, D.O. Gunter, G.W. Crabtree, W. Zhong, U. Balachandran, P. Haldar, R.S. Sokolowski, V.K. Vlasko-Vlasov, and V.I. Nikitenko, *Nature* **376**, 44 (1995).
- <sup>5</sup> Y. Iijima, N. Tanabe, O. Kohno, and Y. Ikeno, *Appl. Phys. Lett.* **60**, 769 (1992).
- <sup>6</sup> X.D. Wu, S.R. Foltyn, P.N. Arendt, W.R. Blumenthal, I.H. Campbell, J.D. Cotton, J.Y. Coulter, W.L. Hults, M.P. Maley, H.F. Safar, and J.L. Smith, *Appl. Phys. Lett.* **67**, 2397 (1995).
- <sup>7</sup> D.P. Norton, A. Goyal, J.D. Budai, D.K. Christen, D.M. Kroeger, E.D. Specht, Q. He, B. Saffian, M. Paranthaman, C.E. Klabunde, D.F. Lee, B.C. Sales, and F.A. List, To appear in *Science* Nov. 1, 1996.
- <sup>8</sup> A.E. Pashitski, A. Gurevich, A.A. Polyanskii, D.C. Larbalestier, A. Goyal, E.D. Specht, D.M. Kroeger, J.A. DeLuca and L.E. Tkaczyk, Submitted (1996).
- <sup>9</sup> Th. Schuster, H. Kuhn, A. Weißhardt, H. Kronmuller, B. Roas, O. Eibl, M. Leghissa, and H.-W. Neumuller, *Appl. Phys. Lett.* **69**, 1954 (1996).
- <sup>10</sup> J.A. Parrell, A.A. Polyanskii, A.E. Pashitski, and D.C. Larbalestier, *Supercond. Sci. and Technol.* **9**, 393 (1996).
- <sup>11</sup> M. Polak, J.A. Parrell, A.A. Polyanskii, A.E. Pashitski, and D.C. Larbalestier, Submitted to *Appl. Phys. Lett.* (Aug. 1996).
- <sup>12</sup> D.A. Korzekwa, J.F. Bingert, E.J. Podtburg, and P. Miles, *Appl. Supercond.* **2**, 261 (1994).